

# Dispersion Polymerization of Methyl Methacrylate Stabilized with Poly(1,1-dihydroperfluorooctyl acrylate) in Supercritical Carbon Dioxide

Yu-Ling Hsiao, Elise E. Maury, and Joseph M. DeSimone\*

Department of Chemistry, CB #3290, Venable and Kenan Laboratories, University of North Carolina at Chapel Hill, Chapel Hill, North Carolina 27599-3290

Simon Mawson and Keith P. Johnston

Department of Chemical Engineering, University of Texas at Austin, Austin, Texas 78712-1062

Received June 20, 1995; Revised Manuscript Received September 5, 1995\*

**ABSTRACT:** The reaction parameters and progress of the dispersion polymerization of methyl methacrylate (MMA) utilizing poly(1,1-dihydroperfluorooctyl acrylate) [poly(FOA)] as a polymeric stabilizer in supercritical CO<sub>2</sub> were investigated. Spherical and relatively uniform polymer particles were formed. Poly(methyl methacrylate) (PMMA) latex particles with diameters ranging from 1.55 to 2.86  $\mu\text{m}$  were obtained with poly(FOA) stabilizer [ $M_w = 1.0 (\pm 0.4) \times 10^6 \text{ g/mol}$ ] concentration from 16 to 0.24 wt %. Investigations of the particle size and conversion as a function of reaction time indicate that a gel effect occurs between 1 and 2 h of reaction time. In addition, the particle diameter increases with an increase in monomer concentration, presumably due to an increase in the solvency of the reaction medium. Dispersion polymerizations of MMA carried out under different pressures (145–331 bar) produced latex particles with similar diameters, molecular weights, and yields, suggesting that the results are insensitive to the pressure under the reaction conditions investigated. In addition, the phase behaviors of poly(FOA) were thoroughly investigated. Cloud point experiments indicate lower critical solution temperature (LCST) phase behavior for the poly(FOA)/CO<sub>2</sub> system with much higher polymer solubilities than for hydrocarbon polymers.

## Introduction

Recently we reported the successful dispersion polymerization in an inert supercritical fluid.<sup>1</sup> We demonstrated that using a fluorinated polymeric surfactant, poly(1,1-dihydroperfluorooctyl acrylate) [poly(FOA)], a stable dispersion of poly(methyl methacrylate) (PMMA) in supercritical CO<sub>2</sub> was formed. Coupled with the successful homogeneous free-radical polymerization of fluorinated monomers in supercritical CO<sub>2</sub>,<sup>2</sup> conducting polymerizations in supercritical CO<sub>2</sub> offers great potential for polymer manufacturing processes in the plastics industry. In addition, due to the unique properties of supercritical fluids,<sup>3</sup> the solvency of the medium can be easily controlled by changing the density of the reaction medium through temperature and pressure profiling. This is in contrast to conventional systems where mixed solvents are used to tune the solvency of the reaction medium. Furthermore, lattice fluid self-consistent field theory has been used to show that the compressibility of the solvent has a significant influence on latex stability in a supercritical fluid due to the entropy gain in removing solvent from the latex surface.<sup>4</sup>

Motivated by the surface coating applications, dispersion polymerization was invented to prepare polymer particles with diameters in the micrometer range.<sup>5</sup> As defined by Barrett,<sup>5,6</sup> a dispersion polymerization is a heterogeneous polymerization process by which latex particles are formed in the presence of a suitable stabilizer from an initially homogeneous reaction mixture. Reaction occurs initially through a solution phase polymerization to produce oligomeric radicals. As these oligomeric radicals grow to a critical chain length, they

precipitate from the solution and undergo aggregative nucleation with other oligomeric radicals and association with the steric stabilizer to form the stable nuclei. At this point, the number of particles is fixed and the particles have a fairly narrow size distribution. Polymerization then takes place primarily in the monomer swollen particle phase as these particles rapidly capture the oligomeric radicals formed in the dispersion medium.<sup>5–7</sup>

The kinetics of dispersion polymerization can be described initially (less than 1% conversion) as a solution phase polymerization.<sup>6</sup> As soon as stable nuclei are formed, polymerization occurs within the polymer particles and the reaction follows the kinetics of bulk polymerization, taking into account the gel effect (Trommsdorff acceleration), partitioning of monomer in the particle phase and the continuous phase, the volume fraction of particles, and plasticization effects.<sup>6</sup>

Polymeric materials can be categorized as either CO<sub>2</sub>-philic or CO<sub>2</sub>-phobic based on their solubility characteristics.<sup>1</sup> Amorphous fluoropolymers or low-melting fluoropolymers and polysiloxanes are soluble in CO<sub>2</sub>,<sup>2,8–15</sup> while most other polymeric materials<sup>3,16</sup> are insoluble in CO<sub>2</sub>. As such, these materials are defined as CO<sub>2</sub>-philic and CO<sub>2</sub>-phobic, respectively. Poly(FOA) is suitable as a polymeric stabilizer in CO<sub>2</sub> due to its surface-active nature in the PMMA-CO<sub>2</sub> system.<sup>1</sup> This amphipathic polymeric stabilizer contains an acrylic-like backbone (CO<sub>2</sub>-phobic) which functions as an anchoring unit that can either physically adsorb or chemically graft onto the growing PMMA particles, while the fluorinated side groups (CO<sub>2</sub>-philic) extend the chain trajectory into the continuous phase, preventing the flocculation of particles through a steric stabilization mechanism.<sup>17,18</sup>

\* Author to whom correspondence should be addressed.

© Abstract published in *Advance ACS Abstracts*, October 15, 1995.

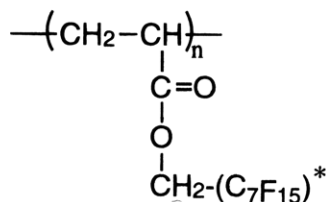


**Figure 1.** Structure of poly(FOA) in CO<sub>2</sub>. \*Note: there are significant numbers of CF<sub>3</sub> branches in the perfluorinated side chains (ca. 25% branches per CF<sub>2</sub> unit).

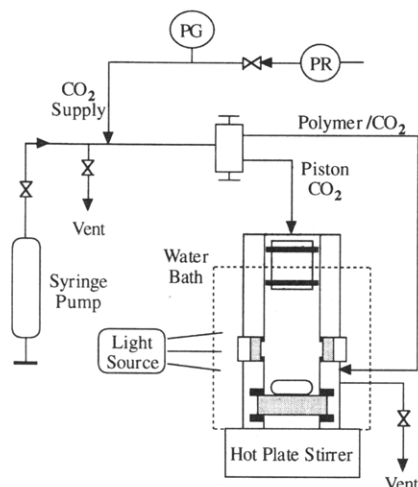


**Figure 2.** Schematic of the variable volume view cell used for the study of poly(FOA)/CO<sub>2</sub> phase behavior. PG = pressure gauge; PR = pressure regulator.

The objective of the collaborative work presented here is to address issues such as the effect of reaction parameters on the dispersion polymerization of methyl methacrylate (MMA) in CO<sub>2</sub> and the function of the poly(FOA) stabilizer in CO<sub>2</sub>. Because the phase behavior of the stabilizer is known to play a key role in steric stabilization, cloud points are presented for poly(FOA) in the temperature and pressure range of interest. This study should provide useful insights into conducting free-radical dispersion polymerizations in CO<sub>2</sub>.

## Experimental Section

**Materials.** Methyl methacrylate (MMA) (Aldrich) was passed through a column of alumina oxide to remove the inhibitor and was deoxygenated before use. 2,2'-Azobisisobutyronitrile (AIBN) (Eastman Kodak) was recrystallized twice from methanol. Tetrahydrofuran (THF) and methanol (Mallinckrodt, HPLC grade) were used as received. Analytical grade or SFC/SFE grade CO<sub>2</sub> was obtained from Air Products and Chemicals and used with a helium head pressure (129 bar).<sup>19</sup> Poly(FOA) was prepared by a solution free-radical polymerization in supercritical CO<sub>2</sub> as previously described.<sup>2</sup> The chemical structure of poly(FOA) is shown in Figure 1.

**Poly(FOA) Phase Behavior Studies.** A schematic of the experimental variable volume view cell used for the poly(FOA)/CO<sub>2</sub> phase equilibria measurements is shown in Figure 2. A view cell containing two sapphire windows (3/8 in. diameter by 1/8 in. thick) with a 180° orientation was used in conjunction with an incandescent light source to backlight the poly(FOA) solution. As shown in Figure 2, the view cell was assembled in a vertical position so that the stir bar (Fisher Scientific Model 14-511-98H) rotated on a flat surface. The agitation was observed to be superior to that obtained with a horizontally assembled view cell and a smaller, egg-shaped stir bar.<sup>14</sup>

Cloud points due to fluid → liquid + liquid phase separation were observed visually as the pressure was slowly reduced at 0.068–0.136 bar/s. The cloud point was defined as the point where the solution turned slightly translucent.<sup>14,20</sup> This

definition is different from that used in the study by Meilchen *et al.* where the cloud point was defined as the point at which it was no longer possible to observe the stir bar.<sup>21</sup> In our studies, initial phase separation and complete turbidity were separated by ±3–5 bar for all reported conditions. For reproducing consistent cloud point measurements, the pressure of the agitated polymer solution was increased to more than 10 bar above the cloud point until the solution became transparent. At this point, agitation was discontinued and the cloud point was again determined. Each cloud point condition was repeated several times with a reproducibility within ±2 bar.

**Dispersion Polymerization.** All dispersion polymerizations were carried out in a 10-mL stainless steel high pressure view cell<sup>22</sup> containing a magnetic stir bar. In a typical polymerization reaction, the initiator (4.9 × 10<sup>-2</sup> mmol of AIBN) and the polymeric stabilizer [poly(FOA)] were charged into the cell, which was then purged with argon for 15 min. The MMA was deoxygenated by purging with argon for 15 min and was injected into the cell under an argon atmosphere. The cell was then filled with liquid CO<sub>2</sub> to ca. 145 bar by using an ISCO syringe pump. The cell was gradually heated to 65 °C and the pressure was increased to 345 bar by gradual addition of CO<sub>2</sub>. The polymerizations were allowed to proceed for reaction times varying from 1 to 4 h. At the end of the polymerization, the reactor was immersed in a cold water bath and the CO<sub>2</sub> was vented immediately through a needle valve into methanol to collect a sample of intact polymer particles that sprayed out of the reaction cell. In polymerizations conducted without an added stabilizer, a large amount of monomer remained and therefore the polymer was recovered by dissolving the cell contents in THF and precipitating this solution into a large excess of methanol. The resulting polymer was washed several times with methanol and dried *in vacuo* at room temperature overnight. In the case of polymerizations conducted with an added stabilizer, the polymer product was collected as a dry white powder and could be removed from the reaction vessel directly. However, in order to quantify the reaction yields, the reaction cell was rinsed with THF to remove any residual PMMA which was isolated by precipitation with methanol.<sup>23</sup> The resulting product was then dried *in vacuo* at room temperature overnight. The polymer conversion was determined gravimetrically. The weight of poly(FOA) was subtracted from the total mass of the product to obtain the weight of PMMA assuming that all of poly(FOA) remained in the cell after the CO<sub>2</sub> was vented.

**Supercritical Fluid Extraction.** Extractions were conducted with an ISCO SFX 2–10 supercritical fluid extractor operated with an ISCO syringe pump (Model 260D). Each sample (ca. 300 mg) was subject to a dynamic extraction for 5–8 h. Liquid CO<sub>2</sub> (344 bar, room temperature), 500 mL, with a flow rate of 1–2 mL/min was used in each extraction. Efficiency of the extraction was tested with a control experiment where 17.2 mg of poly(FOA) was subject to 2 h of extraction under identical conditions; 99.4% of the poly(FOA) was removed after 2 h of extraction.

**Polymer Characterization.** Molecular weights of polymers were determined by using a Waters 150-CV gel permeation chromatography (GPC) with Ultrastaygel columns of 100, 500, 10<sup>3</sup>, and 10<sup>4</sup> Å porosities, using tetrahydrofuran as an eluent against polystyrene standards. Scanning electron micrographs (SEMs) were obtained on a ETEC-Autoscan SEM instrument. The particle-size histograms were constructed by measuring 100–200 individual particles from the electron micrographs, and the number-average particle size and particle size distribution were determined.<sup>24</sup> In the case where PMMA particles exhibit bimodal particle size distribution, both the primary and the secondary particle size are reported and the particle size distribution of the entire sample is calculated. Elemental analysis results were obtained from Galbraith Laboratories, Knoxville, TN.

## Results and Discussion

**Phase Behavior of Poly(FOA) in CO<sub>2</sub>.** Figure 3 shows the experimental cloud point curves of poly(FOA)

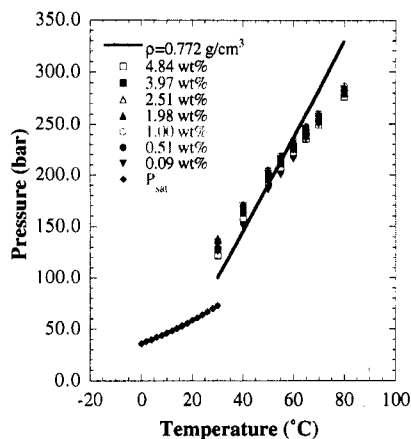


**Figure 3.** Experimental results of poly(FOA) [ $M_w = 1.0 (\pm 0.4) \times 10^6$  g/mol] cloud point behavior in  $\text{CO}_2$ . Above each curve is the one-phase region and below the curve is the two-phase region.

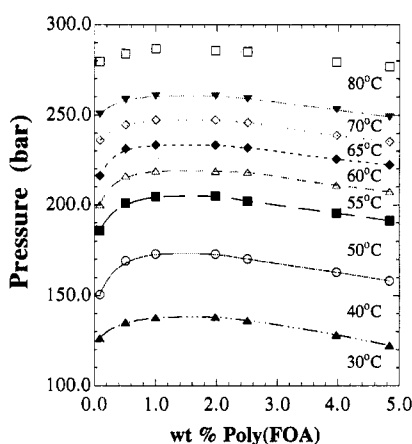


**Figure 4.** Experimental poly(FOA) [ $M_w = 1.0 (\pm 0.4) \times 10^6$  g/mol]  $P$ - $x$  isotherms showing upper critical solution pressure phase behavior in  $\text{CO}_2$ . The curves connect the experimental data.

[ $M_w = 1.0 (\pm 0.4) \times 10^6$  g/mol, determined by small-angle neutron scattering technique<sup>25</sup>] in  $\text{CO}_2$  with concentrations varying from 0.09 to 4.84 wt %. The vapor pressure curve for pure  $\text{CO}_2$  is also shown along with a  $0.772 \text{ g/cm}^3$  isochore. The cloud point slope,  $(\partial P / \partial T)_x$ , is positive, indicating lower critical solution temperature (LCST) phase behavior, which is common to a variety of SCF/polymer systems.<sup>14,20,21,26</sup> The poly(FOA)/ $\text{CO}_2$  cloud point slope changes from 2.95 to 3.09 bar/ $^\circ\text{C}$  across the critical point of  $\text{CO}_2$ . These values are comparable to the cloud point slopes of PMMA in chlorodifluoromethane (2.8 bar/ $^\circ\text{C}$ )<sup>20</sup> and poly(1,1,2,2-tetrahydroperfluoroalkyl acrylate) [poly(TAN), with an average alkyl chain length of 9.6] in  $\text{CO}_2$  (3.01–3.21 bar/ $^\circ\text{C}$ ).<sup>14</sup>

Figures 4 and 5 show several pressure–concentration ( $P$ - $x$ ) isotherms and temperature–concentration ( $T$ - $x$ ) isobars, respectively. The curves are similar in shape for all conditions studied. The critical point, i.e., upper critical solution pressure or lower critical solution temperature, is between 1.0 and 2.0 wt % poly(FOA) in each case, although determination of an exact critical concentration is difficult due to the flatness of the isobar or isotherm. The pressure necessary to maintain the poly(FOA) solution in the one-phase region is observed to increase with increasing temperatures as expected in order to maintain the high density of the medium. Note that the cloud point deviates slightly from the

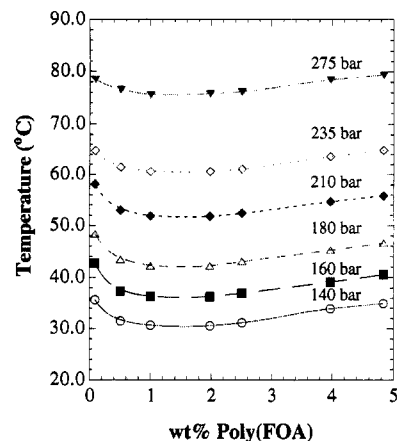


**Figure 5.** Experimental poly(FOA) [ $M_w = 1.0 (\pm 0.4) \times 10^6$  g/mol]  $T$ - $x$  isobars showing LCST phase behavior in  $\text{CO}_2$ . The curves connect the experimental data.

$0.772 \text{ g/cm}^3$  isochore shown in Figure 3 and that this high molecular weight polymer represents one of the most  $\text{CO}_2$ -soluble polymers ever reported.

LCST phase separation is entropically driven and is a consequence of the large difference between the free volume of poly(FOA) and the highly compressible  $\text{CO}_2$ .<sup>27</sup> Because  $\text{CO}_2$  is more compressible than poly(FOA), an increase in temperature or decrease in pressure will cause a larger expansion of  $\text{CO}_2$  than the polymer. As the  $\text{CO}_2$  expands, it gains free volume and entropy. This results in an increase in the poly(FOA)–poly(FOA) segmental interactions due to localized densification. At the phase separation temperature or cloud point, the solution free energy is minimized by an entropically driven phase separation, which results in the formation of two liquid phases, i.e., a poly(FOA)-enriched phase and a  $\text{CO}_2$ -rich phase. An analysis of the two phase region of either Figure 4 or 5 reveals that the poly(FOA)-enriched phase contains a significant amount of  $\text{CO}_2$ , i.e., > 90%.

**Dispersion Polymerization of MMA in  $\text{CO}_2$ .** (1) **Effect of the Concentration of Poly(FOA).** Polymerizations utilizing high molecular weight poly(FOA) [ $M_w = 1.0 (\pm 0.4) \times 10^6$  g/mol] as a steric stabilizer were conducted at high pressure ( $\sim 340$  bar) in order to ensure the initial homogeneity of the reaction mixture. The cloud point experiments indicate that poly(FOA) is soluble in pure  $\text{CO}_2$  at this pressure. Although MMA is a nonsolvent for poly(FOA), preliminary studies suggest that poly(FOA) in a mixture of the polar MMA monomer and the nonpolar  $\text{CO}_2$  results in a solution with a larger second virial coefficient ( $A_2$ ) than that observed for poly(FOA) and pure  $\text{CO}_2$ .<sup>28</sup>

We have previously shown that the initiator efficiency for AIBN is 1.5 times higher in  $\text{CO}_2$  than in benzene due to a minimal solvent cage effect.<sup>29</sup> The dispersion polymerization of MMA stabilized with poly(FOA) and initiated with AIBN provides an efficient system to produce polymers with high yields and molecular weights in  $\text{CO}_2$ .<sup>1</sup> Table 1 summarizes further systematic studies based on the dispersion polymerizations of MMA (21 w/v % in  $\text{CO}_2$ ) using various amounts of the polymeric stabilizer [poly(FOA)]. Spherical particles with diameters from 2.86 to  $1.55 \mu\text{m}$  were obtained.

In the absence of a steric stabilizer, polymerization of MMA in  $\text{CO}_2$  for 4 h yielded a coagulum with a relatively low molecular weight (Table 1). In sharp contrast to the control experiment conducted without stabilizer, the dispersion polymerization carried out in

**Table 1. Effect of the Concentration of Poly(FOA) (21 w/v % MMA, 4 h)**

poly(FOA), <sup>a</sup> wt %	yield, <sup>b</sup> %	$M_n$ , kg/mol	$M_w/M_n$	particle size, <sup>c</sup> $\mu\text{m}$	PSD <sup>d</sup>
0	47	85	3.72		
0.24	86	255	2.40	2.86	1.17
0.47	90	259	2.53	2.49 (2.35) <sup>e</sup>	1.01
1.2	89	252	2.56	2.08 (2.07) <sup>e</sup>	1.01
2.3	84	231	2.69	2.43 (2.46) <sup>e</sup>	1.03
4.5	92	316	2.09	2.44	1.02
8.7	89	230	2.51	1.64	1.21
16	90	293	2.33	1.55, 0.93 <sup>f</sup>	1.08

<sup>a</sup> Based on monomer plus poly(FOA). <sup>b</sup> Yields obtained from repeated polymerizations are within  $\pm 3\%$ . <sup>c</sup>  $D_n$ , number-average diameter, particle size obtained from repeated polymerizations are within  $\pm 0.03 \mu\text{m}$ , with the exception of the reaction carried out with 0.47 wt % poly(FOA) where the difference is  $0.14 \mu\text{m}$ . <sup>d</sup> PSD (particle size distribution) =  $D_w/D_n$ . <sup>e</sup> Numbers in the parentheses are particle sizes obtained from different runs. <sup>f</sup> PMMA particles exhibit bimodal particle size distribution. Both primary and secondary particle diameters are reported.

the presence of 0.24 wt % (based on MMA) of poly(FOA) produced PMMA latex particles with an increased yield and molecular weight. In addition, the very low amount of the polymeric stabilizer required for a successful dispersion polymerization indicates the high amphiphilicity and strong anchoring effect of poly(FOA) in the PMMA-CO<sub>2</sub> system.

As shown in Table 1, the particle diameter is only slightly affected by the concentration of the stabilizer. Although the decreasing particle size with increasing poly(FOA) concentration does not appear monotonic, the diameter of the particles decreases from 2.86 to 1.55  $\mu\text{m}$  when the concentration of poly(FOA) increases from 0.24 to 16 wt %. In the presence of a large amount of poly(FOA), it is believed that the oligomeric PMMA radicals can rapidly adsorb the stabilizer prior to aggregation with other particles. As a result, there is an increase of the number of stable nuclei with higher stabilizer content and correspondingly smaller particles are produced.<sup>30</sup>

The slightly smaller particles obtained in the polymerization conducted with 1.2 wt % poly(FOA) (Table 1) may be the result of a change in the contribution of the anchoring modes of poly(FOA) to the PMMA particle. There are two proposed nonionic stabilization mechanisms, steric and depletion stabilization.<sup>17,31,32</sup> Within the steric stabilization mechanism, several modes of stabilizer anchoring are possible, including adsorption, absorption, and grafting.<sup>17</sup> It has been difficult to distinguish between these modes of anchoring experimentally. Nevertheless, there have been reports on elucidating the different anchoring modes by isolating the grafted and the ungrafted products.<sup>32-35</sup> In some systems where amphipathic block copolymers were used as stabilizers, grafting in addition to physical adsorption was suggested to explain the increased affinity of the stabilizers in these systems, which subsequently resulted in a broader or bimodal particle size distribution.<sup>36</sup> During the polymerization of MMA, poly(FOA) may become chemically grafted onto the PMMA particles, presumably through chain transfer reactions with the poly(FOA) backbone. In the presence of different amounts of poly(FOA), the extent of the physical adsorption, absorption, and chemical grafting could vary. The particle diameters are thus determined by the relative contribution of these anchoring modes.

Supercritical CO<sub>2</sub> extractions were carried out on PMMA particles synthesized with various concentra-

**Table 2. Supercritical Fluid Extraction of PMMA Particles**

poly(FOA) in the feed, wt %	elem anal results poly(FOA), wt %		% poly(FOA) remaining <sup>a</sup>	surface coverage, <sup>b</sup> mg/m <sup>2</sup>
	before extraction	after extraction		
0.47	0.30	0.14	30%	0.69
1.2	1.0	0.40	33%	1.65
2.3	1.9	0.53	23%	2.56
16	16	2.7	17%	8.15

<sup>a</sup> Values were calculated based on the original amount of poly(FOA) in the feed. The residual poly(FOA) probably exists as a graft copolymer. <sup>b</sup> Coverage of the grafting was calculated based on the particle diameter and the residual amount of poly(FOA).

tions of poly(FOA). The results of the extractions are shown in Table 2. Elemental analysis results indicate that the concentration of poly(FOA) before extraction is slightly lower than that in the feed. This could be attributed to some loss of poly(FOA) when the CO<sub>2</sub> was vented from the cell. The residual amounts of poly(FOA) on the PMMA particles range from 33% to 17% of the original feed amount. This suggests either that poly(FOA) was strongly adsorbed on PMMA or partially encapsulated in the PMMA particles and the amount of CO<sub>2</sub> used in the extraction was not enough to remove it or that some degree of grafting occurs during the polymerization of MMA and that the resulting poly(FOA)-g-PMMA exhibits poor solubility in CO<sub>2</sub> and could not be removed even after extensive extraction. The calculated coverages of the steric stabilizer based on the residual poly(FOA) and particle diameters range from 0.69 to 8.15 mg/m<sup>2</sup>, which fall within the range of the calculated grafting coverages of surfactants that have been reported.<sup>37,38</sup> The range of surface coverage reflects both the difference in total particle surface area and the level of grafting under various poly(FOA) concentrations. Grafting of poly(FOA) on the PMMA particles could occur in the solution phase early in the polymerization process possibly through chain transfer of the growing PMMA chain to the backbone of the stabilizer to generate secondary or tertiary carbon radicals. The methylene linkage on the side chain of poly(FOA) is less susceptible to hydrogen abstraction by a free-radical mechanism due to the strong electronegativity of the adjacent CF<sub>2</sub> units. As sufficient graft copolymers were generated, stable nuclei were formed through association of oligomeric radicals with the graft copolymers or homopolymers. Polymerization then took place in the particle phase where the extent of further grafting would be significantly reduced. The degree of polymerization of the resulting PMMA remains high, indicating chain transfer reactions do not occur as extensively after the particle phase polymerization takes place. Since the graft copolymer was generated during the polymerization, its structure and amount present could vary with the concentration of stabilizer, which would subsequently affect the diameter of PMMA particles.<sup>35</sup> Although CO<sub>2</sub> is known to plasticize PMMA,<sup>39</sup> the particles obtained after the supercritical CO<sub>2</sub> extraction retained their spherical morphology.<sup>40</sup> This could be attributed to the high melt viscosity of the high molecular weight PMMA particles<sup>41,42</sup> or to the stabilization of the PMMA particles by the residual graft copolymers.

Latex particles stabilized with 0.47–2.3 wt % of poly(FOA) exhibit a narrow particle size distribution (Table 1, Figure 6). The sharp distribution is an indication that the initial nuclei were formed within a short time

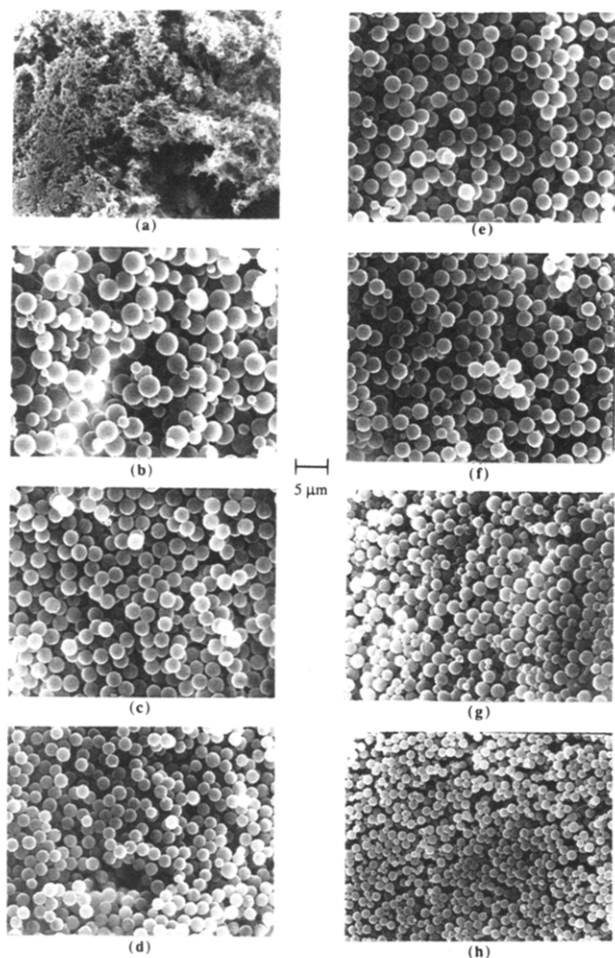


**Figure 6.** SEMs of PMMA latex particles synthesized with 21 w/v % MMA and (a) 0, (b) 0.24, (c) 0.47, (d) 1.2, (e) 2.3, (f) 4.5, (g) 8.7, and (h) 16 wt % poly(FOA).

period and the subsequent particle growth took place without the formation of new nuclei and without agglomeration of particles. In the presence of higher concentrations of polymeric stabilizer, the excess stabilizer is able to stabilize a second crop of smaller particles growing in the solution but not yet captured by the large particles. The histograms of PMMA powders synthesized with 0.47 and 16 wt % poly(FOA) are shown in parts a and b of Figure 7, respectively. A distinct secondary particle formation is observed at the higher stabilizer concentration relative to that obtained at the low stabilizer concentration. The broader particle size distribution found in the polymerization stabilized with 0.24 wt % of poly(FOA) (Table 1) may arise from some degree of coalescence of the incompletely covered particles.<sup>37</sup> With the limited amount of steric stabilizer available to reach the minimum coverage of the particle surface, some degree of coalescence would result, causing a decrease in total surface area.

Dispersion polymerizations of MMA conducted with poly(FOA) concentration higher than 2.3 wt % formed stable dispersions throughout the entire reaction times and were obtained as powdery materials. With concentrations of poly(FOA) at 2.3 wt % or lower, the dispersions were initially stable but subsequently settled before the reactions were completed. Polymers obtained from these reactions were recovered as solid chunks which could be easily broken apart into powdery polymers. The poly(FOA) must continue to provide steric stabilization in the settled particles, otherwise the highly plasticized particles would become agglomerated

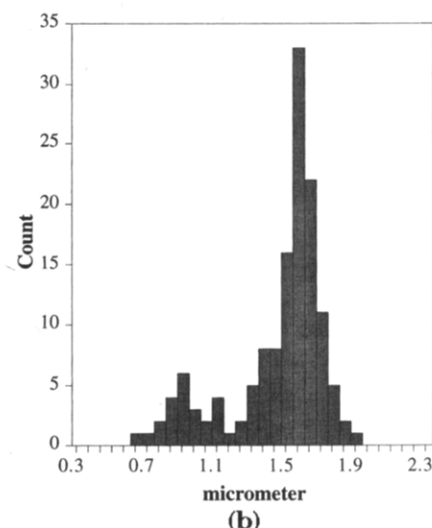
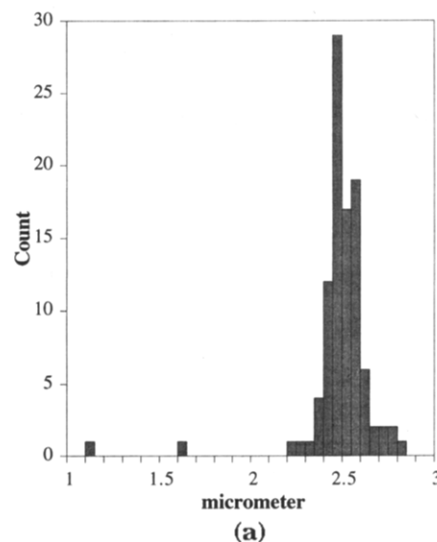


**Figure 7.** (a) Particle size distribution histogram (monomodal) of PMMA (0.47 wt % poly(FOA), 21 w/v % MMA). (b) Particle size distribution histogram (bimodal) of PMMA (16 wt % poly(FOA), 21 w/v % MMA).

in the chunks, resulting in much larger particles and very broad particle size distributions. In addition, supercritical CO<sub>2</sub> must efficiently facilitate the swelling of the PMMA particles with initiator and monomer and allow the polymerization to take place inside the settled particles phase. In all of the reactions shown here, regardless of how long the colloid remained visually stabilized, the addition of a stabilizer results in significant enhancement in the conversion and molecular weight of the resulting PMMA.

**(2) Conversion and Particle Diameter as a Function of Reaction Time.** The reaction progress was monitored by analyzing samples obtained from stopping four different reactions at reaction times of 1, 2, 3, and 4 h. The percent monomer conversion and the particle diameters are shown in Table 3. These polymerization solutions developed an orange opalescence within 3 min after reaching the reaction temperature of 65 °C. This is a result of the Tyndall effect, which arises from the scattering of the transmitted light by colloidal particles. An opaque white latex formed ca. 15 min into the reaction.

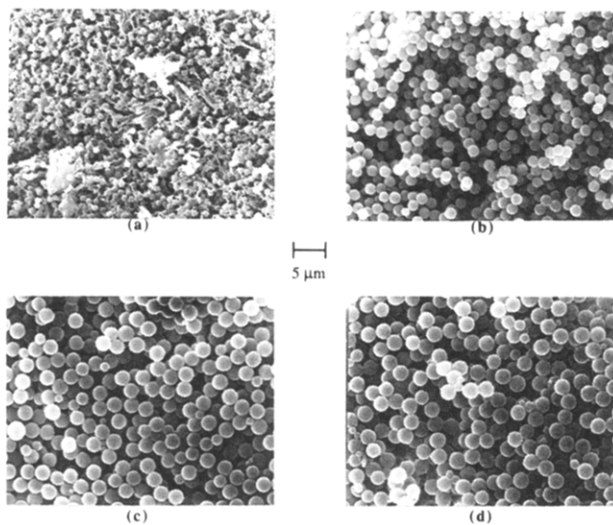
Particles with diameter of 0.91 μm were isolated within 3% overall conversion (Table 3). The morphology of the PMMA particles obtained from 3% conversion



**Table 3. Conversion of MMA as a Function of Time (4.5 wt % Poly(FOA), 21 w/v % MMA)**

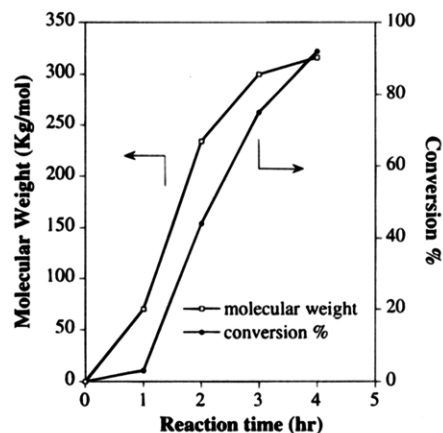
reaction time, h	conversion, %	$M_n$ , kg/mol	$M_w/M_n$	particle size, <sup>a</sup> $\mu\text{m}$	PSD <sup>b</sup>
1	3	70	2.35	0.91	1.02
2	44	234	2.05	1.65	1.02
3	75	300	2.16	2.27	1.03
4	92	316	2.09	2.44	1.02

<sup>a</sup>  $D_n$ , number-average diameter. <sup>b</sup> PSD (particle size distribution) =  $D_w/D_n$ .

**Figure 8.** SEMs of PMMA latex particles obtained from reactions conducted with 21 w/v % MMA and 4.5 wt % poly(FOA) at (a) 1 h, (b) 2 h, (c) 3 h, and (d) 4 h.

exhibits partially irregular structure due to the difficulty in isolating the particles in the presence of a large excess of residual monomer, which is a good solvent for the PMMA particles (Figure 8a). Nevertheless, after 1 h into the reaction, the particle size distribution was already nearly monodisperse, suggesting that the formation of a new crop of particles must fall to a negligible level at the early stage of the polymerization. Barrett *et al.* suggested that initially stabilized nuclei are probably less than 0.01  $\mu\text{m}$  in diameter. This nucleation stage is completed very rapidly, well under 1% conversion.<sup>6</sup> This statement is consistent with our observation as well as results by others.<sup>5-7,34,43,44</sup>

A gel effect (autoacceleration) seems to begin to play a role somewhere between 1 h (3% conversion) and 2 h (44% conversion) as indicated by the sharp increase in the number-average molecular weight during this time period (Figure 9). This is similar to what is typically observed in common organic solvents where a gel effect occurs between 20 and 80% conversion for dispersion polymerizations.<sup>5</sup> Once the particles are formed, it is believed that the polymerization takes place primarily in the monomer swollen particles. Polymerization in highly viscous particles results in a gel effect which leads to an increase in the rate of polymerization and an increase in the molecular weight of the polymer. Although the gel effect arises from the retardation of termination rate relative to the propagation rate, at high polymer conversions even monomer diffusion is hindered in many cases. However, due to the ability of  $\text{CO}_2$  to plasticize PMMA,<sup>3,39</sup> polymerizations carried out in  $\text{CO}_2$  offer the advantage of increasing the diffusivity of monomers into the growing polymer particles to maintain a sufficient rate of propagation, which in turn effectively facilitates the gel effect. The molecular weight of the polymer reached a plateau ca. 3 h into

**Figure 9.** PMMA molecular weight and conversion as a function of reaction time.

the reaction. The tailing-off of the polymerization rate as well as the molecular weight corresponds to a gradual diminution in the residual monomer content at high conversion.

**(3) Effect of the Monomer Concentration.** Dispersion polymerizations of methyl methacrylate were also carried out at three different monomer concentrations. Control reactions conducted in the absence of steric stabilizers at the three different initial monomer concentrations all afforded PMMA with lower yields, lower molecular weights, and broader molecular weight distributions (Table 4). Table 4 also summarizes the results of the dispersion polymerization of MMA carried out at a constant molarity of poly(FOA)<sup>45</sup> and with 10, 21, and 41 w/v % MMA. The results indicate that the particle diameter and the particle size distribution increase as the concentration of monomer increases. The trend toward increased particle size with increasing monomer concentration appears to be primarily a solvent effect. The solvency of the dispersion medium plays a crucial role in determining the particle sizes of the latices.<sup>6</sup> Similar observations have been made in numerous studies of the effect of solvency on the particle size.<sup>5,7,30,32,34,36,44,46</sup>

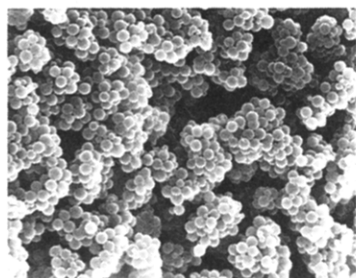
In order to demonstrate the solvency change of the MMA- $\text{CO}_2$  system, first, the critical properties of MMA were estimated by a group contribution technique proposed by Ambrose.<sup>47</sup> The critical temperature, critical pressure, critical volume, and acentric factor for neat MMA were calculated to be 179.85  $^{\circ}\text{C}$ , 36.86 bar, 318.4  $\text{cm}^3/\text{mol}$ , and 0.396, respectively. The critical properties and solubility parameters of the MMA- $\text{CO}_2$  binary system were then obtained from the SF-Solver program that employs a modified Handinson-Brobst-Thomson method<sup>47</sup> and solubility-density relationship.<sup>48</sup> As shown in Table 4, the estimated Hildebrand solubility parameter increases with monomer concentration. Although a more rigorous method using equations of state should give us a better estimation of the critical properties of binary systems, the empirical method that we used in this calculation does provide us a starting place for considering the effect of the solvency in the MMA/ $\text{CO}_2$  system.

The increase in solvency at higher monomer concentration could influence the final particle size and particle size distribution in various aspects. Since PMMA is soluble in its own monomer, for reactions conducted at high initial monomer concentration the critical degree of polymerization at which the oligomeric radicals precipitate from the solution is increased and the

**Table 4. Effect of the Concentration of MMA (Poly(FOA),<sup>a</sup> 4 h)**

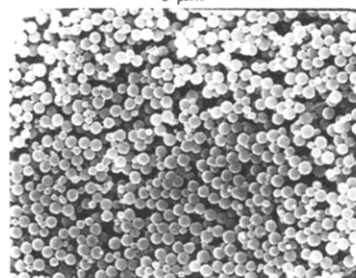
% MMA <sup>b</sup>	Hildebrand parameter, (cal/cm <sup>3</sup> ) <sup>1/2</sup>	stabilizer	yield, %	$M_n$ , kg/mol	$M_w/M_n$	particle size, <sup>c</sup> $\mu\text{m}$	PSD <sup>d</sup>
10	7.178	none	10	23	2.83		
21	7.430	none	47	85	3.72		
41	7.586	none	34	128	4.26		
10		poly(FOA)	84	167	2.26	1.33	1.02
21		poly(FOA)	90	293	2.33	1.55 <sup>e</sup>	1.08
41		poly(FOA)	84	339	2.58	2.61	1.09

<sup>a</sup> The amount of poly(FOA) was held constant relative to the total volume of the solution (400 mg in a 10-mL cell). <sup>b</sup> w/v % in CO<sub>2</sub>. <sup>c</sup>  $D_n$ , number-average diameter. <sup>d</sup> PSD (particle size distribution) =  $D_w/D_n$ . <sup>e</sup> Only primary particle diameter is reported.

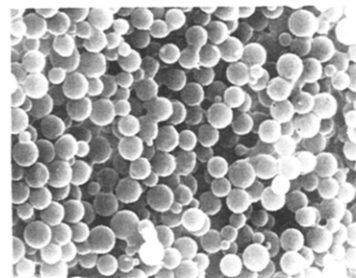


(a)

5  $\mu\text{m}$



(b)



(c)

**Figure 10.** SEMs of PMMA latex particles synthesized with constant amount of poly(FOA)<sup>45</sup> and (a) 10 w/v % MMA, (b) 21 w/v % MMA, and (c) 41 w/v % MMA.

duration of stable nuclei formation is prolonged. In addition, the adsorption efficiency of the polymeric stabilizer decreases with an increase in the solvency of the medium. This results in the formation of fewer nuclei leading to correspondingly larger particles and a wider particle size distribution (Figure 10). The locus of polymerization as well as the partitioning of the monomer in the particle phase versus the solution phase changes with the solvency of the dispersion medium. This also changes the polymerization kinetics of the system.

**(4) Pressure Effect on Dispersion Polymerization of MMA.** The polymerization of MMA using a low molecular weight poly(FOA) ( $M_n = 1.4 \times 10^4$  g/mol, determined by GPC) as the stabilizer and AIBN as the initiator was conducted at four different pressures as

**Table 5. Pressure Study for MMA Polymerization<sup>a</sup> Using Poly(FOA)<sup>b</sup> as the Stabilizer**

initial pressure, bar	final pressure, bar	yield, <sup>c</sup> %	$M_n$ , kg/mol	$M_w/M_n$	particle diameter, $\mu\text{m}$
145	172	92	351	2.5	1.8
193	207	94	322	2.4	1.6
269	255	85	272	2.5	1.6
331	300	88	338	2.4	1.7

<sup>a</sup> 20 w/v % of MMA using AIBN as the initiator. <sup>b</sup> 17 wt % poly(FOA),  $M_n = 1.4 \times 10^4$  g/mol was used. <sup>c</sup> Yields ( $\pm 5\%$ ) were determined gravimetrically.

shown in Table 5. A lower molecular weight poly(FOA) was used to broaden the range of accessible pressures without inducing precipitation of the stabilizer. High yields and molecular weights were achieved in all cases with no apparent trend. The same observation could be made for the particle size. The solvency of the CO<sub>2</sub> can be manipulated by changing the density of the system through varying the temperature and pressure. As the pressure changes from 145 to 331 bar at 65 °C, the density increases from ca. 0.60 to 0.85 g/mL.<sup>49</sup> Low molecular weight poly(FOA) stabilizer exhibits high solubility at low pressures and polymerization could start homogeneously even at 145 bar. Our results suggest that the density or the solvency differences at these four polymerization pressures for this particular system do not significantly affect the polymerization kinetics and the outcome of the reaction.

An interesting observation was made regarding the changes in pressure during polymerizations as shown in Table 5. Polymerizations conducted at 331 and 269 bar resulted in a decrease of pressure of the system by 31 and 14 bar, respectively. The polymerization of MMA has a negative activation volume and the net volume contraction is estimated to be ca. 20% of the original monomer volume.<sup>50,51</sup> Thus a decrease in the system pressure due to a volume contraction is expected. However, the increase in the system pressure when polymerizations were conducted at 145 and 193 bar is unexpected. Beckman *et al.* have recently estimated, *via* theoretical calculations, the amount of CO<sub>2</sub> absorbed by PMMA as a function of pressure.<sup>52</sup> The amount of CO<sub>2</sub> dissolved in the polymer phase increases with pressure. Thus, the fraction of CO<sub>2</sub> residing in the interstitial space or continuous phase for reactions conducted at lower pressures will be higher than for reactions conducted at higher pressures. As the amount of CO<sub>2</sub> used in these systems is roughly the same, the change in reaction pressure might be due to different degrees of partitioning of CO<sub>2</sub> in the continuous phase and particle phase as well as the volume contraction from the polymerization reaction. Further studies will focus on rationalization of these complex pressure changes.

## Conclusion

Cloud point experiments indicate LCST phase behavior for the poly(FOA)/CO<sub>2</sub> system with much higher polymer solubilities than for hydrocarbon polymers. The reaction parameters of the dispersion polymerization of MMA stabilized by poly(FOA) in supercritical CO<sub>2</sub> were investigated. PMMA latex particles from 1.55 to 2.86  $\mu\text{m}$  in diameter are obtained with various concentrations of poly(FOA). Physical adsorption, absorption, and chemical grafting could contribute to the colloidal stability observed during dispersion polymerization of MMA in CO<sub>2</sub>. The particle diameter is found to increase with monomer concentration, presumably due to an increase in the solvency of the reaction medium. The polymerization kinetics observed by following the progress of the dispersion polymerization indicate that a gel effect occurs between 1 and 2 h into the reaction. The gel effect may be facilitated by the plasticization of PMMA with CO<sub>2</sub>, which promotes the transport of monomer into the polymer phase. Dispersion polymerizations of MMA carried out under different pressures (145–331 bar) produced latex particles with similar diameters, suggesting that the particle diameter is insensitive to the reaction pressure under the conditions investigated.

**Acknowledgment.** At UNC, we gratefully acknowledge the financial support from the National Science Foundation for a Presidential Faculty Fellowship (J.M.D.: 1993–1997) as well as from the Consortium on Polymeric Materials Synthesis and Processing in CO<sub>2</sub>, which is sponsored by the National Science Foundation, the Environmental Protection Agency, Du Pont, Hoechst-Celanese, Air Products and Chemicals, B. F. Goodrich, Eastman Chemical, Bayer, Xerox, and General Electric. In addition we thank ISCO Corporation for the donation of a syringe pump and the supercritical fluid extractor. We are also grateful for assistance from Wallace Ambrose at the Dental School of UNC—Chapel Hill SEM facility and Dorian P. Canelas for carrying out GPC analysis. We thank James B. McClain for synthesizing the high molecular weight poly(FOA). At UT, we are grateful for support from NSF (CTS-9218769 and CHE-9315429 with DeSimone), the Texas Advanced Technology Program (3658–198), and the Separations Research Program at the University of Texas.

## References and Notes

- DeSimone, J. M.; Maury, E. E.; Menciloglu, Y. Z.; McClain, J. B.; Romack, T. J.; Combes, J. R. *Science* **1994**, *265*, 356.
- DeSimone, J. M.; Guan, Z.; Elsbernd, C. S. *Science* **1992**, *257*, 945.
- McHugh, M. A.; Krukonis, V. J. *Supercritical Fluid Extraction: Principles and Practice*, 2nd ed.; Butterworth-Heinemann: Stoneham, 1993.
- Peck, D. G.; Johnston, K. P. *Macromolecules* **1993**, *26*, 1537.
- Barrett, K. E. J. *Dispersion Polymerization in Organic Media*; Wiley: London, 1975.
- Barrett, K. E. J.; Thomas, H. R. *J. Polym. Sci. Part A-1* **1969**, *7*, 2621.
- Thomson, B.; Rudin, A.; Lajoie, G. *J. Polym. Sci.: Part A: Polym. Chem.* **1995**, *33*, 345.
- Hoeftling, T. A.; Newman, D. A.; Enick, R. M.; Beckman, E. J. *J. Supercrit. Fluids* **1993**, *6*, 165.
- Combes, J. R.; Guan, Z.; DeSimone, J. M. *Macromolecules* **1994**, *27*, 865.
- DeSimone, J. M.; Romack, T. J.; Combes, J. R. *Macromolecules* **1995**, *28*, 1724.
- DeSimone, J. M.; Guan, Z.; Combes, J. R.; Menciloglu, Y. Z. *Macromolecules* **1993**, *26*, 2663.
- Hoeftling, T.; Stofesky, D.; Reid, M.; Beckman, E.; Enick, R. M. *J. Supercrit. Fluids* **1992**, *5*, 237.
- McFann, G. J. Ph.D. Thesis, University of Texas, 1993.
- Mawson, S. M.; Johnston, K. P.; Combes, J. M.; DeSimone, J. M. *Macromolecules* **1995**, *28*, 3182.
- Tuminello, W. H.; Dee, G. T.; McHugh, M. A. *Macromolecules* **1995**, *28*, 1506.
- Consani, K. A.; Smith, R. D. *J. Supercrit. Fluids* **1990**, *3*, 51.
- Napper, D. H. *Polymeric Stabilization of Colloidal Dispersions*; Academic Press: London, 1983.
- Napper, D. H.; Netschey, A. J. *Colloid Interface Sci.* **1971**, *37*, 528.
- The presence of a helium (He) head space in carbon dioxide could affect the solvency of the continuous phase due to the finite solubility of He in carbon dioxide (5.7 mol % of He in carbon dioxide at 129 bar of He head pressure).
- Haschets, C. W.; Shine, A. D. *Macromolecules* **1993**, *26*, 5052.
- Meilchen, M. A.; Hasch, B. M.; McHugh, M. A. *Macromolecules* **1991**, *24*, 4974.
- Lemert, R. M.; DeSimone, J. M. *J. Supercrit. Fluids* **1990**, *4*, 186.
- The quantitative removal of polymers from the reaction cell with a solvent was necessarily done here in order to accurately determine the yields. This, however, would obviously not be the way one would do this on a commercial scale.
- Kobayashi, S.; Uyama, H.; Yamamoto, I.; Matsumoto, Y. *Polym. J.* **1990**, *22*, 759.
- McClain, J. B.; Romack, T.; Samulski, E. T.; Londono, D.; Wignall, G.; DeSimone, J. M., manuscript in preparation.
- Kiran, E.; Zhuang, W. *Polymer* **1992**, *33*, 5459.
- Sanchez, I. C. In *Encyclopedia of Physical Science and Technology*; Academic Press, Inc.: London, 1992; Vol. 13, p 153.
- McClain, J. B.; DeSimone, J. M., unpublished results.
- Guan, Z.; Combes, J. R.; Menciloglu, Y. Z.; DeSimone, J. M. *Macromolecules* **1993**, *26*, 2663.
- Winnik, M. A.; Lukas, R.; Chen, W. F.; Furlong, P.; Croucher, M. D. *Makromol. Chem., Macromol. Symp.* **1987**, *10/11*, 483.
- Feigin, R. I.; Napper, D. H. *J. Colloid Interface Sci.* **1980**, *75*, 525.
- Stejskal, J.; Kratochvil, P.; Konák, C. *Polymer* **1991**, *32*, 2435.
- Paine, A. J. *J. Colloid Interface Sci.* **1990**, *138*, 157.
- Paine, A. J.; Luymes, W.; McNulty, J. *Macromolecules* **1990**, *23*, 3104.
- Shen, S.; Sudol, E. D.; El-Aasser, M. S. *J. Polym. Sci., Part A: Polym. Chem.* **1994**, *32*, 1087.
- Kawaguchi, S.; Winnik, M.; Ito, K. *Macromolecules* **1995**, *28*, 1159.
- Paine, A. J. *Macromolecules* **1990**, *23*, 3109.
- Paine, A. J.; Deslandes, Y.; Gerroir, P.; Henrissat, B. *J. Colloid Interface Sci.* **1990**, *138*, 170.
- Condo, P. D.; Paul, D. R.; Johnston, K. P. *Macromolecules* **1994**, *27*, 365.
- Shaffer, K. A.; DeSimone, J. M. *Trends Polym. Sci.* **1995**, *3*, 146.
- O'Connor, K. M.; Schollosky, K. M. *Polymer* **1989**, *30*, 461.
- Graessley, W. W. *Adv. Polym. Sci.* **1974**, *16*, 1.
- Fitch, R. M.; Prenosil, M. B. *J. Polym. Sci.: Part C* **1969**, *27*, 95.
- Almog, M.; Reich, S.; Levy, M. *Br. Polym. Sci. J.* **1982**, *14*, 131.
- The amount of poly(FOA) used in each run was held constant (400 mg in a 10-mL high-pressure cell, 0.088 mol/L). The concentrations of poly(FOA) represented in weight percent based on monomer are 29, 16, and 8.9 wt % for Table 4 with increasing monomer concentrations.
- Williamson, B.; Lukas, R.; Winnik, M. A.; Croucher, M. D. *J. Colloid Interface Sci.* **1987**, *119*, 559.
- Reid, R. C.; Sherwood, T. K. *The Properties of Gases and Liquids*, 4th ed.; McGraw-Hill: New York, 1987.
- Hildebrand, J. H.; Scott, R. L. *The Solubilities of Nonelectrolytes*, 3rd ed.; Reinhold Publishing Corp.: New York, 1950.
- Guan, Z. Ph.D. Thesis, University of North Carolina, 1994.
- Beuermann, S.; Buback, M.; Russell, G. T. *Macromol. Rapid Commun.* **1994**, *15*, 351.
- Odian, G. *Principles of Polymerization*, 3rd ed.; Wiley: New York, 1993.
- Goel, S. K.; Beckman, E. J. *Polym. Eng. Sci.* **1994**, *34*, 1137.

MA950877W